

Sodium-Carbonate-Assisted Supercritical Water Oxidation of Chlorinated Waste

Poongunran Muthukumaran and Ram B. Gupta*

Department of Chemical Engineering, Auburn University, Auburn, Alabama 36849-5127

Supercritical water oxidation (SCWO) is emerging as a promising technology for the destruction of organic wastes. However, corrosion is a severe problem for chlorinated wastes because of the formation of hydrochloric acid. Recently, it was proposed that the addition of Na_2CO_3 significantly reduces the corrosion. This work examines the effect of Na_2CO_3 on the oxidation kinetics of phenol and 2-chlorophenol in supercritical water. The kinetics data in the absence of Na_2CO_3 are verified to conform to the literature data. New data in the presence of Na_2CO_3 show that the oxidation is highly enhanced, which may be due to a combination of the catalytic effects of Na_2CO_3 and removal of HCl by Na_2CO_3 . If all other kinetic parameters are unchanged, the activation energy of 2-chlorophenol decomposition decreases from 11.5 kcal/mol without Na_2CO_3 to 2.44 kcal/mol with Na_2CO_3 . Similarly, a reduction from 10.4 to 7.5 kcal/mol is observed for phenol. Also, Na_2CO_3 plays a key role in reducing corrosion on the reactor walls by first neutralizing the acid and then providing a large surface area for adsorption of the precipitated corrosive compounds. Because Na_2CO_3 is insoluble in supercritical water, it precipitates as fine particles with a large surface area. A new reactor design is proposed for obtaining fine Na_2CO_3 particles based on the supercritical anti-solvent method; these fine particles provide a surface area that is several orders of magnitude larger than that of the reactor walls.

Introduction

Toxic organic materials are a cause of increasing concern to human society. The significant amounts of organic wastes produced every day are gradually exceeding the capacities of the existing landfills. Although landfills and incineration have conventionally been used for the disposal of organic wastes, these processes have resulted in extensive contamination of both ground-water and the atmosphere. For example, incineration of chlorinated waste is suspected to produce extremely toxic dioxins. Supercritical water oxidation (SCWO) has been gaining importance as a feasible hazardous waste disposal technique.^{1–9} In this technique, water at high temperatures (above 374 °C) and high pressures (above 221 bar) is used as a medium for spontaneous oxidation of the hazardous waste. Under these conditions, water is completely miscible with organic materials and oxygen, and it has a low viscosity and high mass transfer rates. Several studies have demonstrated that oxidation efficiencies of 99.99% or higher can easily be achieved within less than a minute of reaction time.^{7,9–11} It has been estimated that U.S. industry produces about 600,000 tons of chlorinated waste for disposal every year, and the military has weapon chemicals to be disposed that have heterogeneous atoms including Cl, S, and N.^{12–15} Also, there are numerous potential space and defense applications involving heterogeneous atoms that can utilize this technology.^{13,16–19}

Because of the importance of chlorinated waste, its SCWO has been examined by several groups.^{20,21} Yang and Eckert² studied the destruction kinetics of *p*-chlorophenol with a homogeneous catalyst; Jin et al.²² studied the catalytic oxidation of 1,4-dichlorobenzene;

and Li et al.²³ studied 2-chlorophenol oxidation and provided a global kinetic model. Unfortunately, SCWO of chlorinated wastes has a severe corrosion problem because of the formation of hydrochloric acid.^{24–26} In our laboratory, we have also observed that a stainless steel 316 surface can easily be corroded by chlorinated wastes, as shown in Figures 1 and 2. (In Figure 1, a passive protection layer is seen, whereas in Figure 2, this layer is broken in merely 4 h of exposure to a SCWO reaction for 2-chlorophenol). This difficulty with corrosion led to the use of more expensive alternate reactor materials such as titanium or Inconel.^{12,24} However, the problem of corrosion still remains. In later efforts, NaOH was added to neutralize the acid, but corrosion persisted because of the resulting sticky NaCl. Several inorganic salts were also tried because of their interesting solubility properties in water.⁷ These salts are highly soluble in ambient water but insoluble under supercritical conditions because of the low dielectric constant²⁷ of supercritical water (Figure 3).²⁸

Several researchers have studied the catalytic effect of the salts: Song et al.²⁹ studied several alkali salts for their catalytic activity for steam char gasification; Minowa et al.³⁰ provided a detailed description of cellulose liquefaction using Na_2CO_3 catalyst in hot compressed water at different temperatures; Levent and Ayse³¹ demonstrated the use of sodium carbonate as a catalyst for the pyrolysis of used sunflower oil; and Lee et al.³² used alkali carbonates including Na_2CO_3 with nickel as a catalyst and observed the highest increase in gas yield for the Na_2CO_3 case. These studies suggest that there is a good potential for Na_2CO_3 being used as a catalyst in the SCWO process.

Recently, Ross et al.²⁵ tested several inorganic salts and concluded that the addition of Na_2CO_3 can enhance reaction rates and reduce the corrosion significantly for SCWO oxidation of *p*-dichlorobenzene and hexachloroben-

* Author to whom correspondence should be addressed.
E-mail: gupta@auburn.edu. Tel.: (334) 844-2013. Fax: (334) 844-2063.

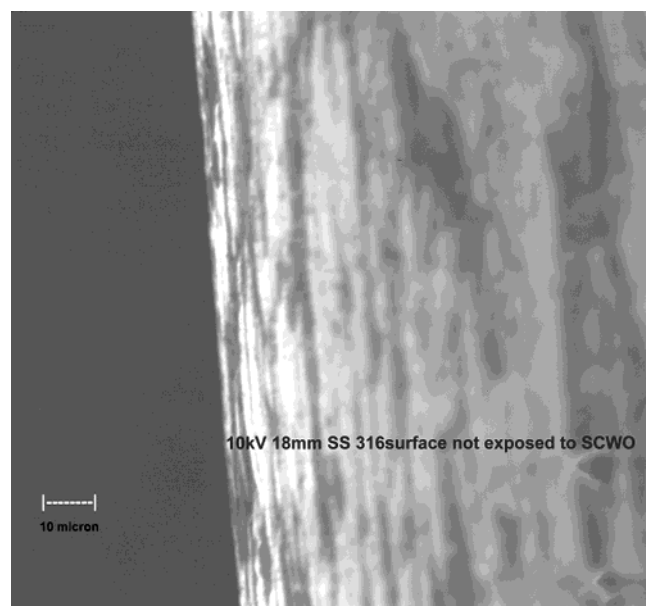


Figure 1. SEM picture of stainless steel 316 surface not exposed to SCWO. Passivation layer is seen here.

zene. In a later work, Ross et al.³³ modified the process in which Na_2CO_3 was placed in the reactor and heated prior to the addition of water and organic materials. In contrast to other inorganic salts, the solubility variation of Na_2CO_3 is rapid with temperature, especially around the critical temperature of water (374 °C). As a result, Na_2CO_3 precipitates as fine particles and provides large surface area for the adsorption of NaCl (formed by the reaction of HCl with Na_2CO_3). This reduces the exposure of both HCl and NaCl to the reactor wall and, hence, also reduces the corrosion significantly. It is to be noted here that Na_2CO_3 is inexpensive and commercially available. These preliminary experiments were conducted in batch reactors, and a fluidized bed reactor scheme was proposed.²⁵ Additional studies on the continuous-flow reactor and on the kinetics of oxidation are needed for a better understanding of the process.

This work examines the effect of the addition of Na_2CO_3 on the continuous-flow SCWO reactor. Oxidation kinetics for 2-chlorophenol and phenol are studied. The process is further explored to see how corrosion protection is enhanced with even low amounts of Na_2CO_3 in the feed.

Experimental Section

Apparatus and Procedure. The SCW oxidation reactions were conducted in a high-pressure, isothermal, isobaric flow reactor at 400 °C and 240–300 bar with residence times from 20 to 80 s. Plug-flow operation was chosen because of its simplicity in carrying out kinetic experiments involving organic compounds that can be dissolved in water in the concentration range of interest. Another reason for choosing plug-flow operation as opposed to batch operation is that it uses fresh Na_2CO_3 continuously, providing “newly formed” surface available throughout the reaction. The schematic diagram of the apparatus is given in Figure 4. The reactor has two feed streams: (a) organic waste (phenol or 2-chlorophenol) dissolved in water with or without sodium carbonate and (b) hydrogen peroxide (0.3 vol %) dissolved in water. A double-piston metering pump (Eldex AA 100S) was used to pump the two feed streams separately. The liquid levels in the feed tanks were

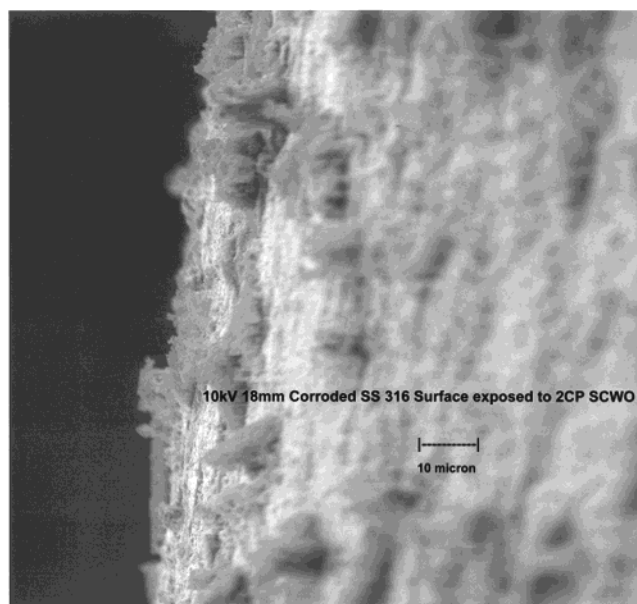


Figure 2. SEM picture of stainless steel 316 surface exposed to conventional SCWO of 2-chlorophenol for 4 h. Passivation layer is broken because of corrosion.

measured throughout the experiments to ensure the accuracy of the feed flow rates into the system, and flow rates were determined from this information. Both feed streams were preheated using $\frac{1}{8}$ -in. stainless steel (SS 316) tubings of about 5.5 m in length. Then, the streams were mixed at the reactor entrance using a tee joint. The reactor is made of SS 316 with an i.d. of $\frac{1}{4}$ -in. and a volume of 10 mL. The reactor/preheater assembly was placed in a constant-temperature furnace (Thermolyne 30400). The effluent from the reactor was cooled using a heat exchanger. The reactor temperature was measured using Omega K-type cement-on thermocouples and controlled to within 3 °C of the set value. The pressure was measured at two different points within an accuracy of 3.5 bar and controlled using a back-pressure regulator (GO Regulator, Inc., Corona, CA; $P_{\text{max}} = 350$ bar) placed after the heat exchanger. Safety rupture disks rated at 340 bar were installed in the feed streams. After passing through the back-pressure regulator, effluent was separated into liquid and gas streams using a glass gas–liquid separator, and then the products were taken for analysis. The concentration of Na_2CO_3 used was low enough that plugging was avoided in the reactor, the downstream tubings, and the back-pressure regulator. Fine-sized Na_2CO_3 particles would also have been a reason for no plugging in the reactor and the downstream tubing. After the product mixture is cooled in the heat exchanger, Na_2CO_3 will dissolve back into water, which avoids plugging of the back-pressure regulator. The extent of decomposition of H_2O_2 was tested by pumping 0.3 vol % H_2O_2 alone into the reactor and then analyzing the effluents; in all cases, full decomposition of H_2O_2 was observed. The residence time was primarily varied by changing the feed flow rates. In addition, changing the pressure also produced some residence time variations.

Chemical Analysis. The liquid effluents were analyzed with a high-performance liquid-chromatographic system (Waters 600 with Millennium Chromatography Manager) using a C-18 reverse-phase column (Novapak C18). The mobile phase was an equivalent mixture of methanol and water at a 1 mL/min flow rate. Compo-

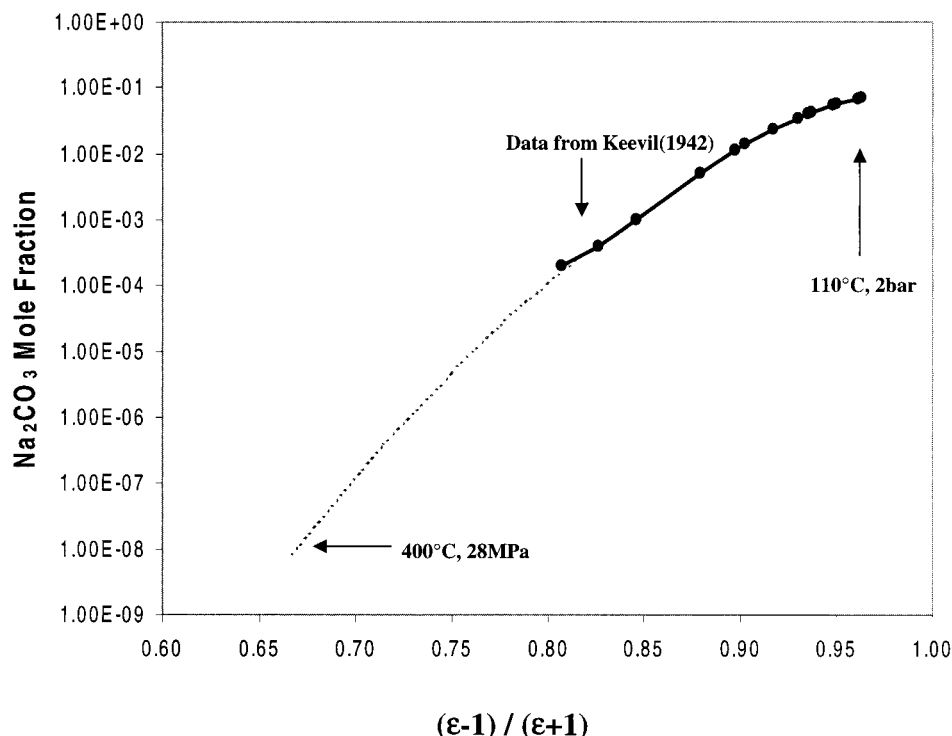


Figure 3. Sodium carbonate solubility in water versus dielectric constant function $(\epsilon - 1)/(\epsilon + 1)$.

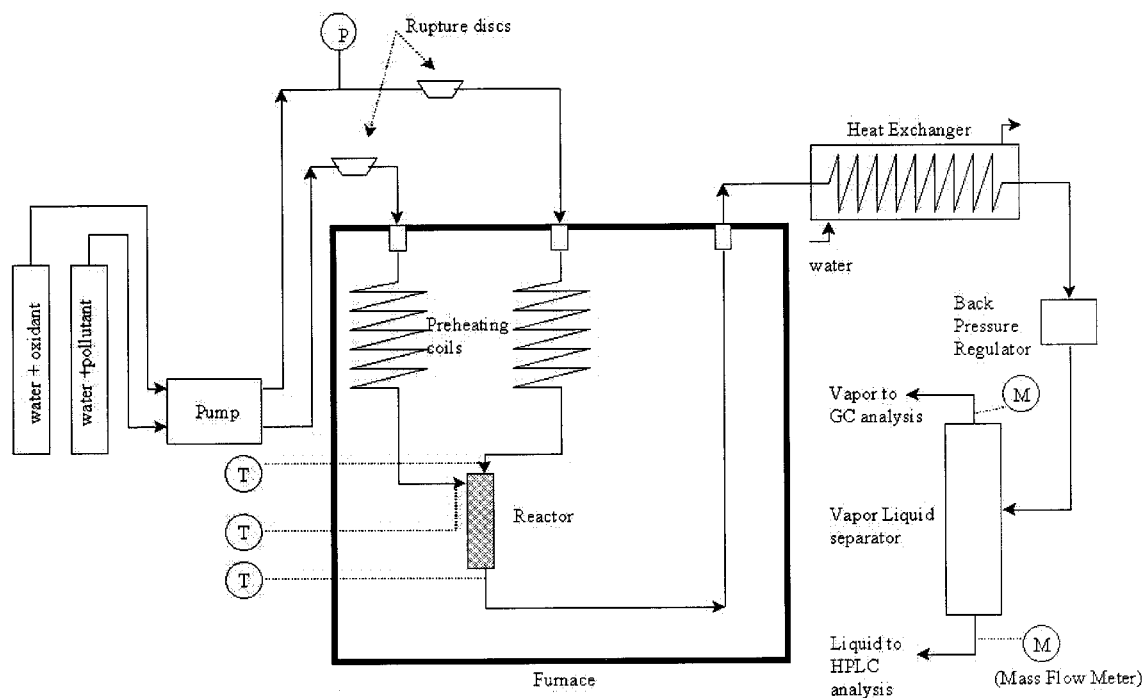


Figure 4. Apparatus for supercritical water oxidation.

nents were detected using a UV detector (Waters 2487) set at 270 nm. The kinetic data obtained are based on the disappearance of the phenol or 2-chlorophenol.

Error Analysis. The feed flows were measured with less than 5% error. In the analysis using HPLC, each sample was injected multiple times to ensure that the readings have less than 5% error. Temperature was controlled to within 2 °C and pressure to within 3.5 bar (50 psi).

Results and Discussion

Results for the oxidation of 2-chlorophenol without Na_2CO_3 are shown in Table 1. The feed composition of

2-chlorophenol was about 100 mg/L. The hydrogen peroxide feed concentration (3 g/L) was much higher than the stoichiometric requirement. The residence time (t_R) at the reactor temperature (T) and pressure (P) is calculated as

$$t_R = \frac{\text{Reactor Volume}}{[\text{Mass Flowrate} \times \text{Specific Volume}(T, P)]} \quad (1)$$

About 50% oxidation of 2-chlorophenol is achieved in 30 s, and 99% in about 60 s of reaction time. These kinetic results agree with the previous data of Li et al.²³ Upon addition of Na_2CO_3 in the feed, the reaction rates

Table 1. Experimental Data for SCW Oxidation of 2-Chlorophenol without Na₂CO₃

mass flow rate (g/min)	<i>P</i> (bar)	<i>T</i> (°C)	<i>t_R</i> (s)	<i>y</i> _{2CP,in}	<i>y</i> _{H2O2,in}	<i>y</i> _{H2O,in}	% conversion (<i>X</i> _{2CP} × 100)
3.78	252	404	25.3	6.98×10^{-6}	4.75×10^{-4}	0.9995	72.1
4.66	276	402	29.2	6.81×10^{-6}	4.75×10^{-4}	0.9995	59.3
4.88	269	401	25.9	7.03×10^{-6}	4.75×10^{-4}	0.9995	51.7
4.86	264	401	24.1	6.75×10^{-6}	4.75×10^{-4}	0.9995	44.7
4.60	264	401	25.4	6.70×10^{-6}	4.75×10^{-4}	0.9995	41.7
4.91	252	401	20.4	6.87×10^{-6}	4.75×10^{-4}	0.9995	36.7
3.70	260	396	34.4	5.51×10^{-6}	4.75×10^{-4}	0.9994	74.6
3.00	257	395	40.2	6.84×10^{-6}	4.75×10^{-4}	0.9996	63.0
3.00	254	394	40.7	7.51×10^{-6}	4.75×10^{-4}	0.9996	61.7
2.88	226	395	28.3	7.72×10^{-6}	4.75×10^{-4}	0.9997	54.3
3.38	255	395	36.1	7.18×10^{-6}	4.75×10^{-4}	0.9996	39.2
4.00	248	396	26.3	7.18×10^{-6}	4.75×10^{-4}	0.9996	45.2
4.00	257	395	31.5	7.18×10^{-6}	4.75×10^{-4}	0.9996	51.9
4.00	259	395	31.9	7.18×10^{-6}	4.75×10^{-4}	0.9996	56.3
4.80	253	395	24.0	7.18×10^{-6}	4.75×10^{-4}	0.9996	38.1
4.80	255	395	25.0	7.18×10^{-6}	4.75×10^{-4}	0.9996	36.7
5.00	259	395	25.6	7.18×10^{-6}	4.75×10^{-4}	0.9996	70.4
6.00	262	398	20.9	7.18×10^{-6}	4.75×10^{-4}	0.9996	33.0
5.99	259	396	21.0	6.83×10^{-6}	4.75×10^{-4}	0.9996	28.6
6.66	260	394	21.0	7.18×10^{-6}	4.75×10^{-4}	0.9996	32.1
5.60	255	395	21.8	8.00×10^{-6}	4.75×10^{-4}	0.9997	44.5
6.50	255	398	17.1	7.54×10^{-6}	4.75×10^{-4}	0.9997	28.2
7.60	255	393	16.9	7.37×10^{-6}	4.75×10^{-4}	0.9996	11.1
5.20	310	400	45.7	7.54×10^{-6}	4.75×10^{-4}	0.9997	85.9
5.50	310	401	42.0	7.64×10^{-6}	4.75×10^{-4}	0.9997	80.4
6.50	310	398	38.1	7.54×10^{-6}	4.75×10^{-4}	0.9997	87.0
6.40	310	400	36.6	7.00×10^{-6}	4.75×10^{-4}	0.9996	86.2
7.33	312	399	33.7	7.64×10^{-6}	4.75×10^{-4}	0.9997	87.6
7.13	314	395	37.9	7.29×10^{-6}	4.75×10^{-4}	0.9996	86.7
4.50	312	403	48.4	7.78×10^{-6}	4.75×10^{-4}	0.9997	80.4
3.42	303	400	64.3	8.19×10^{-6}	4.75×10^{-4}	0.9997	87.3
3.33	307	398	72.5	8.41×10^{-6}	4.75×10^{-4}	0.9997	89.1

Table 2. Experimental Data for SCW Oxidation of 2-chlorophenol with Na₂CO₃

mass flow rate (g/min)	<i>P</i> (bar)	<i>T</i> (°C)	<i>t_R</i> (s)	<i>y</i> _{2CP,in}	<i>y</i> _{H2O2,in}	<i>y</i> _{H2O,in}	Na ₂ CO ₃ mg/kg	% conversion (<i>X</i> _{2CP} × 100)
5.50	265	399	23.0	7.95×10^{-6}	4.72×10^{-4}	0.9995	688	97.0
5.66	248	403	16.5	9.42×10^{-6}	6.63×10^{-4}	0.9993	535	96.6
4.40	234	401	18.9	7.95×10^{-6}	4.72×10^{-4}	0.9995	688	97.4
5.20	246	401	18.1	7.84×10^{-6}	4.60×10^{-4}	0.9995	699	97.5
4.90	278	401	29.6	8.62×10^{-6}	5.56×10^{-4}	0.9994	618	97.3
3.66	271	401	35.4	6.21×10^{-6}	2.88×10^{-4}	0.9997	436	97.5
3.91	272	402	33.0	5.89×10^{-6}	2.59×10^{-4}	0.9997	453	98.0
4.05	272	401	32.9	7.01×10^{-6}	3.68×10^{-4}	0.9996	394	99.4
5.01	276	400	29.1	8.49×10^{-6}	4.83×10^{-4}	0.9995	23	88.8
4.85	276	402	28.5	8.76×10^{-6}	5.14×10^{-4}	0.9995	22	89.6
4.75	257	402	28.0	8.66×10^{-6}	5.01×10^{-4}	0.9995	22	87.4
4.85	272	402	26.6	8.61×10^{-6}	4.95×10^{-4}	0.9995	22	90.3
4.93	272	401	21.4	8.53×10^{-6}	4.87×10^{-4}	0.9995	22	90.6
4.88	262	402	22.9	8.40×10^{-6}	4.72×10^{-4}	0.9995	10	77.8
3.75	261	402	29.4	8.21×10^{-6}	4.51×10^{-4}	0.9995	11	76.6
4.99	262	402	22.4	8.21×10^{-6}	4.51×10^{-4}	0.9995	11	76.5
4.00	255	402	25.6	7.70×10^{-6}	3.97×10^{-4}	0.9996	12	58.4
7.33	255	394	16.9	6.74×10^{-6}	3.28×10^{-4}	0.9997	56	96.2
8.66	262	398	14.2	6.86×10^{-6}	3.39×10^{-4}	0.9997	55	96.1
8.66	262	395	15.8	7.99×10^{-6}	4.60×10^{-4}	0.9995	48	96.2
6.66	253	395	17.5	7.42×10^{-6}	3.97×10^{-4}	0.9996	52	97.3
5.33	259	398	21.9	6.49×10^{-6}	3.03×10^{-4}	0.9997	58	98.2
4.40	252	400	23.1	6.75×10^{-6}	3.28×10^{-4}	0.9997	56	97.2
3.53	252	400	28.8	6.43×10^{-6}	2.98×10^{-4}	0.9997	58	97.5
3.42	279	403	41.4	6.16×10^{-6}	2.74×10^{-4}	0.9997	60	99.5
4.40	276	402	31.5	6.75×10^{-6}	3.28×10^{-4}	0.9997	56	99.3
5.50	279	400	28.2	6.75×10^{-6}	3.28×10^{-4}	0.9997	56	99.2
6.50	278	399	24.1	6.85×10^{-6}	3.38×10^{-4}	0.9997	55	98.5
7.33	281	398	23.7	6.74×10^{-6}	3.28×10^{-4}	0.9997	56	98.4
8.00	279	395	24.3	7.42×10^{-6}	3.97×10^{-4}	0.9996	52	97.5

are enhanced significantly. Experiments were performed for 10, 20, 55, 400, and 650 mg/kg loadings of Na₂CO₃ in the feed (Table 2). Even the small amount of 10 mg/kg Na₂CO₃ provided a noticeable increase in

the conversion, which increases with increasing sodium carbonate amount, reaching 99% in 30 s for the 55 mg/kg case. The conversion remains high for the higher loading of Na₂CO₃ (Figure 5).

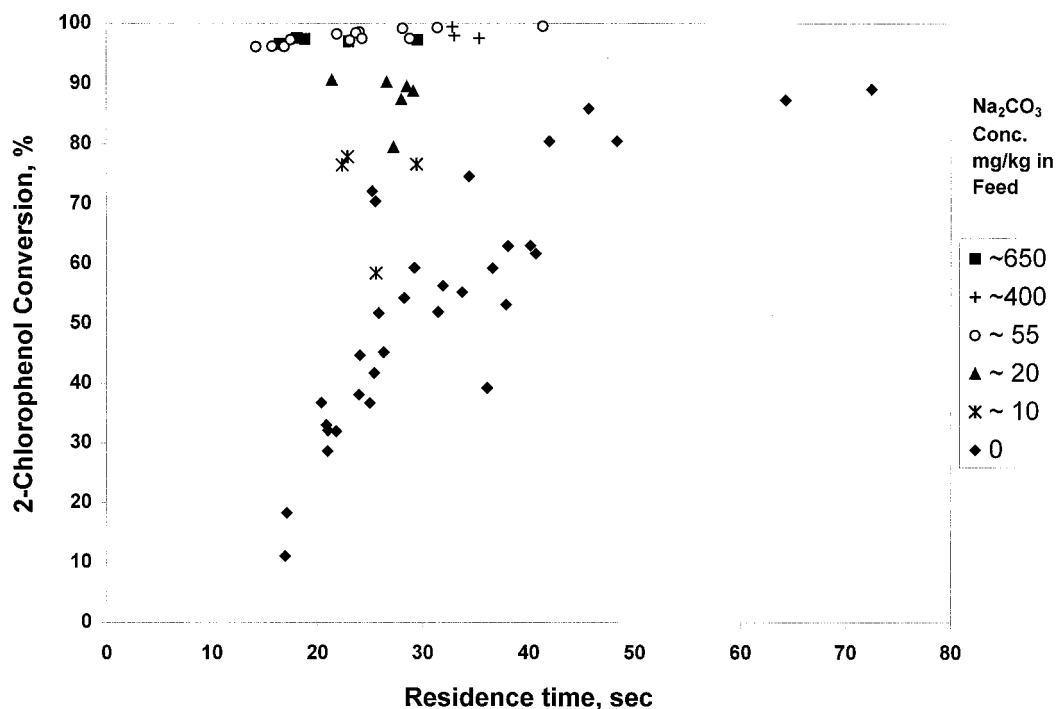


Figure 5. Supercritical water oxidation of 2-chlorophenol with and without Na_2CO_3 .

The significant increase in the rate suggests that Na_2CO_3 enhances one or more steps in the oxidation of 2-chlorophenol. Na_2CO_3 is believed to hydrolyze the chlorine and OH functional groups into phenolates,^{25,33} which are unstable and easily broken into smaller molecules, ultimately converting to CO_2 , water, and NaCl .

To quantify the extent of rate enhancement, a kinetic analysis was performed. For 2-chlorophenol SCW oxidation, Li et al.²³ have derived a global kinetic expression for an isothermal, isobaric, plug-flow reactor

$$-\frac{dC_{2\text{CP}}}{dt_R} = kC_{2\text{CP}}^a C_{\text{O}_2}^b C_{\text{H}_2\text{O}}^c \quad (2)$$

where C_i is the concentration of component i , k is the reaction rate constant, and a , b , and c are the partial orders of the reaction with respect to the 2-chlorophenol, oxygen, and water concentrations, respectively. The above equation can also be written for mole fractions (y_i) and specific molar volume (V°) as^{3,23}

$$-\frac{dy_{2\text{CP}}}{dt_R} = k \left(\frac{1}{V^\circ} \right)^{a+b+c-1} y_{2\text{CP}}^a y_{\text{O}_2}^b y_{\text{H}_2\text{O}}^c \quad (3)$$

For $a \neq 1$, eq 3 is integrated as

$$X_{2\text{CP}} = 1 - \left[1 - A \exp \left(- \frac{E_a}{RT} \right) \left(\frac{1}{V^\circ} \right)^{(a+b+c-1)} (1-a) y_{2\text{CP}}^{a-1} y_{\text{O}_2}^b y_{\text{H}_2\text{O}}^c t_R \right]^{1/(1-a)} \quad (4)$$

where A is the frequency factor, E_a is the activation energy, R is the universal gas constant, T is the reactor temperature in Kelvin, and $X_{2\text{CP}}$ is the extent of conversion written as

$$X_{2\text{CP}} = \frac{y_{2\text{CP},\text{in}} - y_{2\text{CP},\text{out}}}{y_{2\text{CP},\text{in}}} \quad (5)$$

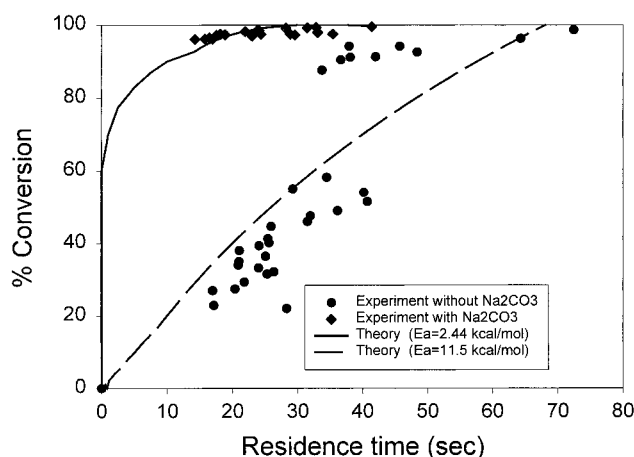


Figure 6. Comparison of 2-chlorophenol experimental conversions (this work) with theory (ref 1). For the experiment with Na_2CO_3 , the sodium carbonate concentrations is 55 mg/kg or higher.

In eq 5, it is assumed that the mixture molar volume is constant, which is a valid assumption. In the integration of eq 3, it is assumed that the feed is very dilute in 2-chlorophenol and oxygen is used in high excess so that the oxygen and water mole fractions remain constant. In fact, the mole fraction of water remains about 0.999 in all of the experiments. Also, all of the experiments were conducted with a large excess of hydrogen peroxide so that the reactor exit oxygen mole fraction could be approximated as the initial oxygen mole fraction. Because hydrogen peroxide was used, the oxygen mole fraction was calculated using appropriate stoichiometry from the complete decomposition of hydrogen peroxide.

The extent of conversion is calculated from eq 3 using the parameters suggested by Li et al.²³ as $a = 0.88 \pm 0.06$, $b = 0.41 \pm 0.12$, $c = 0.34 \pm 0.17$, $A = 10^{2.0 \pm 1.2}$, and $E_a = 11.0 \pm 3.8$ kcal/mol. In the calculations for Figure 6, a value of 11.5 kcal/mol is used, which is in the prescribed range. The comparison of the theoretical conversion to experimental data is shown in Figure 6.

Table 3. Experimental Data for SCWO Oxidation of Phenol with and without Na₂CO₃

mass flow rate (g/min)	<i>P</i> (bar)	<i>T</i> (°C)	<i>t_R</i> (s)	<i>y</i> _{2CP,in}	<i>y</i> _{H2O2,in}	<i>y</i> _{H2O,in}	Na ₂ CO ₃ mg/kg	% conversion (<i>X</i> _{2CP} × 100)
4.40	310	401	51.7	1.08 × 10 ⁻⁵	4.72 × 10 ⁻⁴	0.9995	—	83.5
3.50	317	403	66.0	1.01 × 10 ⁻⁵	5.18 × 10 ⁻⁴	0.9995	—	88.6
2.44	312	398	103.9	1.08 × 10 ⁻⁵	4.72 × 10 ⁻⁴	0.9995	—	78.7
6.00	321	397	44.7	9.85 × 10 ⁻⁶	5.40 × 10 ⁻⁴	0.9995	—	72.6
7.33	321	395	37.9	1.07 × 10 ⁻⁵	4.73 × 10 ⁻⁴	0.9995	—	68.5
7.50	321	394	38.0	1.10 × 10 ⁻⁵	4.51 × 10 ⁻⁴	0.9995	—	63.1
8.00	255	388	21.2	1.18 × 10 ⁻⁵	3.97 × 10 ⁻⁴	0.9996	—	54.3
9.32	248	388	14.7	1.18 × 10 ⁻⁵	3.97 × 10 ⁻⁴	0.9996	—	48.7
4.40	264	396	30.9	1.29 × 10 ⁻⁵	3.28 × 10 ⁻⁴	0.9997	—	70.8
4.44	267	398	30.9	1.07 × 10 ⁻⁵	4.79 × 10 ⁻⁴	0.9995	—	59.6
3.43	262	400	34.1	1.18 × 10 ⁻⁵	3.97 × 10 ⁻⁴	0.9996	—	68.5
4.40	307	400	51.7	1.08 × 10 ⁻⁵	4.72 × 10 ⁻⁴	0.9995	—	72.9
4.66	307	400	48.8	1.18 × 10 ⁻⁵	3.97 × 10 ⁻⁴	0.9996	—	71.0
7.00	307	398	34.5	1.18 × 10 ⁻⁵	3.97 × 10 ⁻⁴	0.9996	—	68.1
6.50	307	395	40.1	1.27 × 10 ⁻⁵	3.38 × 10 ⁻⁴	0.9996	—	65.0
7.33	307	393	37.5	1.07 × 10 ⁻⁵	4.73 × 10 ⁻⁴	0.9995	—	53.6
8.66	310	391	33.0	1.27 × 10 ⁻⁵	3.39 × 10 ⁻⁴	0.9996	—	55.6
3.13	314	406	64.6	1.07 × 10 ⁻⁵	4.74 × 10 ⁻⁴	0.9995	45.37	98.8
3.99	319	398	65.3	9.84 × 10 ⁻⁶	5.41 × 10 ⁻⁴	0.9994	41.60	99.6
5.00	324	400	51.4	9.46 × 10 ⁻⁶	5.71 × 10 ⁻⁴	0.9994	40.00	99.3
6.00	310	400	39.1	9.85 × 10 ⁻⁶	5.40 × 10 ⁻⁴	0.9995	41.67	98.7
7.00	310	395	38.7	1.01 × 10 ⁻⁵	5.18 × 10 ⁻⁴	0.9995	42.86	97.9
7.33	305	392	37.6	1.07 × 10 ⁻⁵	4.73 × 10 ⁻⁴	0.9995	45.43	96.9
9.99	319	392	29.0	1.26 × 10 ⁻⁵	3.45 × 10 ⁻⁴	0.9996	53.35	96.9
8.00	259	391	19.1	1.18 × 10 ⁻⁵	3.97 × 10 ⁻⁴	0.9996	50.00	94.5
6.66	262	392	23.7	9.45 × 10 ⁻⁶	5.72 × 10 ⁻⁴	0.9994	39.94	95.6
5.99	262	395	23.3	1.05 × 10 ⁻⁵	4.90 × 10 ⁻⁴	0.9995	44.41	97.1
8.00	259	395	16.0	1.18 × 10 ⁻⁵	3.97 × 10 ⁻⁴	0.9996	50.00	93.6

Theory agrees qualitatively with the data without any adjustable parameters, predicting the shape and dependence of conversion on residence time. It is noted here that there are some differences in the experimental apparatus of the present work and that of the previous work from which parameters for the calculations were used.

The theory was then applied to oxidation in the presence of sodium carbonate. A homogeneous power law rate expression is assumed for simplicity. A kinetic expression involving the concentration of open sites in the catalyst and adsorption isotherm may be warranted when there is confirmed proof of Na₂CO₃ catalysis. In this work, all of the same kinetic parameters were used as before, except for *E_a*, which was lowered to 2.44 kcal/mol to fit the experimental data at 55 mg/kg Na₂CO₃ and higher loadings. The lowering of *E_a* from 11.5 to 2.44 kcal/mol can be considered an indication of catalytic activity by Na₂CO₃. However, the experimental data can also be fit by keeping all other parameters including *E_a* unchanged and varying the preexponential factor alone. The value of 2.44 kcal/mol was obtained from higher sodium carbonate loading data; a lower loading may provide a higher *E_a* value, but we envision that, for industrial applications, the Na₂CO₃ concentration will be kept at more than 55 mg/kg; hence, the proposed *E_a* of 2.44 kcal/mol is reasonable.

Now it is important to determine whether the rate enhancements by Na₂CO₃ also hold for nonchlorinated compounds. SCWO experiments were conducted to explore the Na₂CO₃ rate enhancement in a nonchlorinated compound, phenol. When phenol/water solution was fed into the reactor with 45 mg/kg Na₂CO₃ and without Na₂CO₃ in separate experiments, we noticed a significant rate enhancement of phenol oxidation (Table 3). In 30 s, the conversion increased from about 50% without Na₂CO₃ to about 98% with Na₂CO₃. To estimate the activation energies, we used the kinetic model proposed by Thornton and Savage,³ which considers

first-order oxidation with respect to the phenol concentration. The extent of conversion, *X_{phenol}* was obtained from

$$X_{\text{phenol}} = 1 - \exp \left[-A \exp \left(\frac{-E_a}{RT} \right) (1/V)^{b+c} J_{\text{H}_2\text{O}}^b J_{\text{O}_2}^c t_R \right] \quad (6)$$

using parameters *A* = 303 M^{-1.2} s⁻¹, *E_a* = 10.4 kcal/mol, *b* = 0.7, and *c* = 0.5. These parameters were adopted from Thornton and Savage,³ but the value of *E_a* was adjusted slightly from their original value of 12.4 kcal/mol to fit our data. Another model for phenol kinetics was published by Krajnc and Levec⁴ using *E_a* = 29.8 kcal/mol, but this value was reported to be nonintrinsic and, hence, was not used here. The parameter adjustment was performed using the optimization routine (Nelder–Mead Simplex algorithm) provided in the Matlab package. The error between the calculated and experimental conversions was minimized by varying *E_a*.

Theory compares well with the experimental data for phenol conversion, and the comparison is shown in Figure 7. For the case of Na₂CO₃, the *E_a* value was lowered to 7.5 kcal/mol to fit the data. Again, this represents a significant rate enhancement by Na₂CO₃ in phenol oxidation. It should be noted here that the same fit can also be obtained by varying the preexponential factor alone and keeping the activation energy unchanged. Although the decrease in the activation energy is less than that in the case of 2-chlorophenol, a significant rate enhancement was noticed. A possible reason for this is that 2-chlorophenol can initiate reaction with Na₂CO₃ at two sites (Cl and OH groups), whereas phenol has only one site (OH group) for initial reaction with Na₂CO₃. Another mechanism, suggested by Ross et al.,^{25,33} is that Na₂CO₃ converts the chlorine group into a hydroxyl group, which can easily be oxidized subsequently in the presence of an oxidant. In

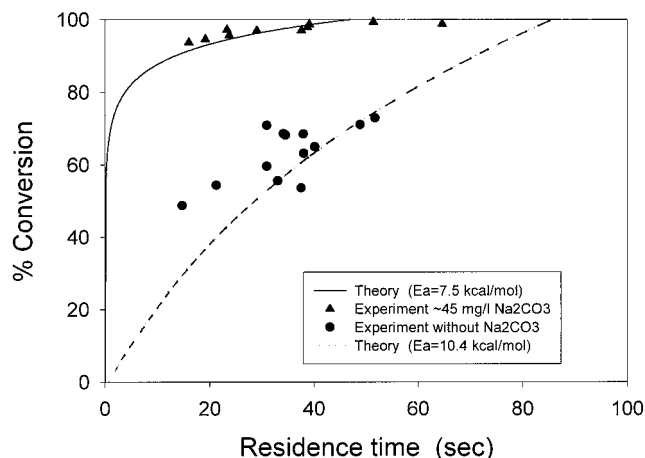


Figure 7. Comparison of phenol experimental conversions (this work) with theory (refs 9 and 10)

such a case, Na_2CO_3 is expected to provide a greater effect on the rate enhancement of 2-chlorophenol than on that of phenol.

In either case, it is envisioned that Na_2CO_3 may act as a catalyst in the aromatic-ring-breaking step and as a reactant in the HCl-neutralizing step. However, more detailed study focusing on the actions of Na_2CO_3 is needed to confirm whether the rate enhancements are due to a combination of the catalytic effects of Na_2CO_3 and removal of HCl by Na_2CO_3 or solely to catalytic effects of Na_2CO_3 . Another interesting point is that, if the rate enhancement is only due to HCl removal, there should not be any rate enhancement in phenol oxidation. A significant rate enhancement in phenol shows that there could be some catalytic effect from Na_2CO_3 .

Clearly, SCWO benefits from the rate enhancement of Na_2CO_3 , as shown here in a continuous-flow reactor, and from the corrosion protection phenomena, as shown by Ross et al.²⁵ in batch reactors. Now the question arises how to obtain high corrosion protection in the continuous-flow process.

Proposed Reactor Design for High Corrosion Protection

The key aspect in corrosion protection is the surface area of the Na_2CO_3 particles. For a given loading of Na_2CO_3 , a higher surface area (smaller particle size) will result in higher corrosion protection. Na_2CO_3 is readily soluble in ambient water, but the solubility decreases as the temperature is raised, and Na_2CO_3 is insoluble in supercritical water (Figure 3). Alternatively, one can envision that the supercritical water acts as a nonsolvent; hence, one can utilize the well-developed supercritical antisolvent technology for fine particle formation.^{34–37} In this technology, because of rapid supersaturation, very fine particles are obtained. In most of the applications, supercritical carbon dioxide is used as the antisolvent to precipitate an organic material from conventional organic solvents. In the proposed reactor design (shown in Figure 8), supercritical water can be used as the antisolvent to precipitate Na_2CO_3 dissolved in cold (e.g., 25 °C) water. It is expected that about 1 μm or smaller Na_2CO_3 particles can be obtained, as is the case for many other solutes in supercritical antisolvent technology.^{34–38}

Assuming the average particle size to be 1 μm , the surface areas of the particles for different loadings of

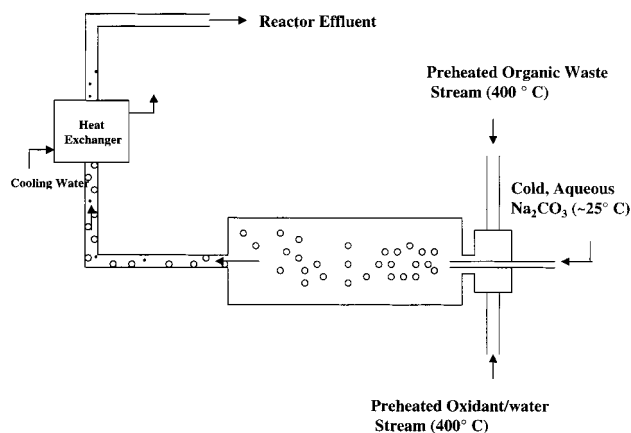


Figure 8. Proposed SCWO reactor that uses supercritical antisolvent technology to obtain a high sodium carbonate particle area for corrosion protection.

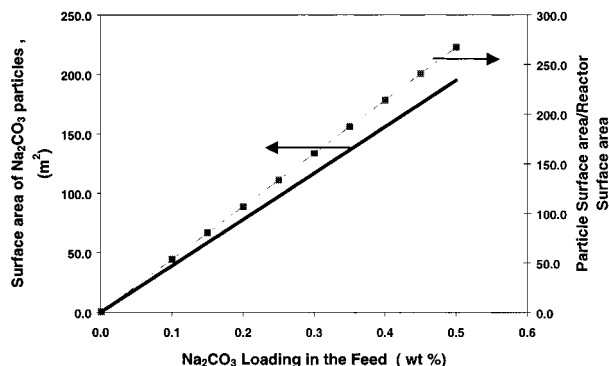


Figure 9. Calculated surface area of Na_2CO_3 particles and ratio of particle surface area to reactor wall area as functions of sodium carbonate loading, based on 1 μm diameter particle size, for a cylindrical reactor (6 in. diameter and 5 ft length) at 400 °C and 300 bar.

Na_2CO_3 in the feed solution are shown in Figure 9. For example, even 0.25 wt % of Na_2CO_3 in the feed results in 97 m^2 of particle surface area. Although the surface area is shown to increase linearly with sodium carbonate loading, in the actual experiment, the increase will be somewhat less than shown here because of particle agglomeration at the higher loadings.

The key factor in corrosion protection is having a much larger particle surface area than the reactor wall area. For illustration, in Figure 9, the surface area ratios are shown for a cylindrical reactor with a diameter of 6 in. and a length of 5 ft for different Na_2CO_3 loadings at 400 °C and 300 bar. A 0.25 wt % loading of sodium carbonate can give a particle surface area that is about 133 times the surface area of the reactor wall. This represents an extremely large corrosion protection in view of adsorption sites for the corrosive species. If the partitioning of the corrosive species between the supercritical fluid and the reactor wall is similar to that between the supercritical fluid and the Na_2CO_3 particles, then the amount of corrosive species depositing on the reactor wall can be reduced by a factor of 133. In practical applications, the Na_2CO_3 concentration is envisioned to be kept large enough to provide for both HCl neutralization and NaCl adsorption and small enough to avoid any plugging. Another issue is the removal of Na_2CO_3 particles from the system. Usually, a supercritical water oxidation reactor is followed by a heat exchanger. When the products are cooled, Na_2CO_3 particles will dissolve back into solution. However, more

research is needed to see how the NaCl and Na₂CO₃ particles behave in the effluent stream inside the supercritical reactor and in the heat exchanger and how they can be transported out of the system.

Conclusion

The oxidation kinetics of 2-chlorophenol and phenol in supercritical water with varying amounts sodium carbonate was studied. The presence of sodium carbonate enhances the oxidation significantly, possibly by lowering the activation energy for both 2-chlorophenol and phenol. However, more research is needed to prove the surface catalysis. Sodium carbonate is not soluble in supercritical water and hence is precipitated as fine particles, which can provide adsorption sites for the corrosive species. A reactor scheme for high corrosion protection is proposed that is based on the supercritical antisolvent particle technology. Calculations show that even small amounts of sodium carbonate can provide a significant particle surface area for corrosion protection.

Acknowledgment

Financial support from the NSF (CST-9801067), NIH (James A. Shannon Director's award to R.B.G.), U.S. Civilian Research and Development Foundation (RCI-170), and NSF-EPSCOR (Young Faculty Career Enhancement Award to R.B.G.) are deeply appreciated. The authors also acknowledge Mr. Joe Aderholdt for his help in constructing the experimental setup.

Literature Cited

- (1) Lin, K.; Wang, P. H. Rate Enhancement by Cations in Supercritical Water Oxidation of 2-Chlorophenol. *Environ. Sci. Technol.* **1999**, *33* (18), 3278–3280.
- (2) Yang, H. H.; Eckert, C. A. Homogeneous catalysis in the Oxidation of *p*-Chlorophenol in Supercritical Water. *Ind. Eng. Chem.* **1988**, *27*, 2009–2014.
- (3) Thornton, T. D.; Savage, P. E. Kinetics of Phenol Oxidation in Supercritical Water. *AIChE J.* **1992**, *38* (3), 321–327.
- (4) Krajnc, M.; Levec, J. On the Kinetics of Phenol Oxidation in Supercritical Water. *AIChE J.* **1996**, *42* (7), 1977–1984.
- (5) Yu, J.; Savage, P. E. Catalytic Oxidation of Phenol over MnO₂ in Supercritical Water. *Ind. Eng. Chem. Res.* **1999**, *38*, 3793–3801.
- (6) Krajnc, M.; Levec, J. Oxidation of Phenol over a Transition-Metal Oxide catalyst in Supercritical Water. *Ind. Eng. Chem. Res.* **1997**, *36*, 3439–3445.
- (7) Tester, J. W.; Holgate, H. R.; Armellini, F. J.; Webley, P. A.; Killilea, W. R.; Hong, G. T.; Barner, H. E. *Supercritical Water Oxidation Technology, Process Development and Fundamental Research*; Tedder, D. W., Pohland, F. G., Eds.; ACS Symposium Series 518, Emerging Technologies in Hazardous Waste Management III; American Chemical Society: Washington, D.C., 1993; pp 35–76.
- (8) Lin, K.-S.; Wang, H. P.; Yang, Y. W. Supercritical water oxidation of 2-chlorophenol effected by Li⁺ and CuO/Zeolites. *Chemosphere* **1999**, *39* (9), 1385–1396.
- (9) Modell, M. Processing Methods for the Oxidation of Organics in Supercritical Water. U.S. Patent 4,338,199, July 6, 1982.
- (10) Koo, M.; Lee, W. K.; Lee, C. H. New reactor system for supercritical water oxidation and its application on phenol destruction. *Chem. Eng. Sci.* **1997**, *52* (7), 1201–1214.
- (11) Gopalan, S.; Savage, P. E. Reaction Mechanism for Phenol Oxidation in Supercritical Water. *J. Phys. Chem.* **1994**, *98* (48), 12646–12652.
- (12) Wagner, M.; Kolarik, V.; Michelfelder, B.; Del Mar Juez-Lorenzo, M.; Hirth, T.; Eisenreich, N.; Eyerer, P. Materials for SCWO processes for the oxidation of chlorine containing residues in supercritical water. *Mater. Corros.* **1999**, *50* (9), 523–526.
- (13) LaJeunesse, C. A.; Haroldsen, B. L.; Rice, S. F.; Brown, B. G. Hydrothermal oxidation of navy shipboard excess hazardous materials; Technical Report SAND97-8212; Sandia National Laboratory: Albuquerque, NM; pp 1–49.
- (14) Cohen, L. S.; Jensen, D.; Lee, G.; Ordway, D. W. Hydrothermal oxidation of Navy excess hazardous materials. *Proc. Int. Conf. Incineration Therm. Treat. Technol.* **1998**, 769–774.
- (15) Soto, M.; Lardis, A. Hydrothermal oxidation (HTO) for the destruction of shipboard wastes. *Proc. Int. Conf. Incineration Therm. Treat. Technol.* **1998**, 753–755.
- (16) Hong, G. T. *Supercritical Water Reactor for Space Applications*; Final Report, Phase 1, NASA Contract No. NAS9-18473, National Aeronautics and Space Administration, U.S. Government Printing Office: Washington, D.C., 1991.
- (17) Hong, G. T.; Killilea, W. R.; Thomason, T. B. Supercritical Water Oxidation: Space Applications; ASCE Space '88 Proceedings, Albuquerque, NM, August 29–31, 1988.
- (18) Elliott, J. P.; Hazlebeck, D. A.; Spritzer, M. H.; Hurley, J. A.; Rising, Stanley A. Hydrothermal Oxidation development for Air Force applications. *Proc. Int. Conf. Incineration Therm. Treat. Technol.* **1999**, 25–29.
- (19) Flesner, R.; Dell'orco, P. C.; Spontarelli, T.; Bishop, R. L.; Skidmore, C. B.; Uher, K.; Kramer, J. F. Pilot-scale base hydrolysis processing of HMX-based plastic-bonded explosives. *NATO Sci. Ser., Ser. 1* **1998**, *22*, 35–45 (Effluents from Alternative Demilitarization Technologies).
- (20) Sorokin, A.; Meunier, B. Efficient H₂O₂ Oxidation of Chlorinated Phenols catalysed by Supported iron Phthalocyanines. *J. Chem. Soc., Chem. Commun.* **1994**, *15*, 1799–1800.
- (21) Lee, D. S.; Gloyna, E. F.; Li, L. Efficiency of hydrogen peroxide and oxygen in supercritical water oxidation of 2,4-dichlorophenol and acetic acid. *J. Supercrit. Fluids* **1990**, *3*(4), 249–55.
- (22) Jin, L.; Ding, Z.; Abraham, M. Catalytic Supercritical Water Oxidation of 1,4-Dichlorobenzene. *Chem. Eng. Sci.* **1992**, *47* (9–11), 2659–2664.
- (23) Li, R.; Savage, P. E.; Szmukler, D. 2-Chlorophenol Oxidation in Supercritical Water: Global Kinetics and Reaction Products. *AIChE J.* **1993**, *39* (1), 178–187.
- (24) Foy, B. R.; Waldthausen, K.; Sedillo, M. A.; Buelow, S. J. Hydrothermal Processing of Chlorinated Hydrocarbons in a Titanium Reactor. *Environ. Sci. Technol.* **1996**, *30*, 2790–2799.
- (25) Ross, D. E.; Jayaweera, I.; Leif, R. N. Method for hot and supercritical water oxidation of material with addition of specific reactants. U.S. Patent 5,837,149, 1998.
- (26) Thomas, A. J., III.; Gloyna, E. F. *Corrosion Behavior of High-Grade Alloys in the Supercritical Water Oxidation of Sludges*; Technical Report No. CRWR229; University of Texas at Austin: Austin, TX, February, 1991.
- (27) Uematsu, M.; Franck, E. U. Static Dielectric Constant of Water and Steam. *J. Phys. Chem. Ref. Data* **1980**, *9* (4), 1291–1305.
- (28) Keevil, N. B. Vapor Pressures of Aqueous Solutions at High Temperatures. *J. Am. Chem. Soc.* **1942**, *64*, 841–850.
- (29) Song, B. H.; Kim, S. Catalytic activity of alkali and iron salt mixtures for steam-char gasification. *Fuel* **1993**, *72* (6), 797–803.
- (30) Minowa, T.; Fang, Z.; Ogi, T.; Varhegyi, G. Liquefaction of cellulose in hot compressed water using sodium carbonate. *J. Chem. Eng. Jpn.* **1997**, *30*, 186.
- (31) Levent, D.; Ayse, A. H. Pyrolysis of used sunflower oil in the presence of sodium carbonate by using fractionating pyrolysis reactor. *Fuel Process. Technol.* **1998**, *57* (2), 81–92.
- (32) Lee, S. W.; Nam, S. S.; Kim, S. B.; Lee, K. W.; Choi, C. S. The effect of Na₂CO₃ on the catalytic gasification of rice straw over nickel catalysts supported on Kieselguhr. *Korean J. Chem. Eng.* **2000**, *17* (2), 174–178.
- (33) Ross, D. E.; Jayaweera, I.; Bomberger, D. C.; Leif, R. N. Hydrothermal oxidation of organic compounds with heterogeneous neutralizing reagent. U.S. Patent 6,010,632, 2000.
- (34) Krukonis, V. J. Supercritical Fluid Processing: Current Research and Operations. In *Proceedings of the International Symposium on Supercritical Fluids*; Perrut, M., Ed.; INPL: Nice, France, 1998; p 541.
- (35) Debenedetti, P. G. Homogeneous Nucleation in Supercritical Fluids. *AIChE J.* **1990**, *35*, 1289.
- (36) Chang, C. J.; Randolph, A. D. Precipitation of Microsize Organic Particles from Supercritical Fluids. *AIChE J.* **1989**, *35*, 1876.

(37) Eckert, C. A.; Knutson, B. L.; Debenedetti, P. G. Supercritical fluids as solvents for chemical and materials processing. *Nature (London)* **1996**, *383* (6598), 313–318.

(38) Chattopadhyay, P.; Gupta, R. B. Supercritical CO₂-Based Production of Fullerene Nanoparticles. *Ind. Eng. Chem. Res.*, **2000**, *39*, 2281–2289.

Received for review May 1, 2000

Revised manuscript received June 29, 2000

Accepted July 10, 2000

IE000447G